15 September 2001

ELSEVIER

Optics Communications 197 (2001) 161–167

OPTICS COMMUNICATIONS

www.elsevier.com/locate/optcom

# Dipole-mode vector solitons in anisotropic photorefractive media

K. Motzek [a,*], A. Stepken [a], F. Kaiser [a], M.R. Belić [b], M. Ahles [c], C. Weilnau [c,d], C. Denz [c,d]

[a] *Institute of Applied Physics, Darmstadt University of Technology, Hochschulstr. 4a, 64289 Darmstadt, Germany*
[b] *Institute of Physics, P.O. Box 57, 11001 Belgrade, Yugoslavia*
[c] *Institute of Applied Physics, Darmstadt University of Technology, Hochschulstr. 6, 64289 Darmstadt, Germany*
[d] *Institute of Applied Physics, Westfälische Wilhelms-Universität Münster, Corrensstr. 2-4, D-48149 Münster, Germany*

Received 24 April 2001; accepted 2 July 2001

**Abstract**

Stable dipole-mode vector solitons in photorefractive (PR) crystals are studied, both in numerical simulations and in experimental investigation. Numerically exact multi-humped solitary solutions to the propagation equations of two incoherently coupled beams in PR media with an anisotropic nonlocal material response are found. A continuous set of dipole-mode vector solitons, ranging from the solitons with negligible dipole-mode contribution to the solitons with negligible ground mode contribution, is identified. The results are compared with experimental data. © 2001 Published by Elsevier Science B.V.

*PACS:* 42.65.Tg; 42.65.Hw

*Keywords:* Vector solitons; Photorefractive media; Nonlinear optics

## 1. Introduction

The prospect of possible use in optical data processing has led to a rising interest in two-transverse-dimensional (2D) optical solitons over the past few years. They have been shown to exist in many different nonlinear materials [1–4] and their interactions have been intensively studied [5–8]. However, spatial solitons in anisotropic photorefractive (PR) media represent a special case, owing to the nonlocal and anisotropic nature of their nonlinearity, which makes the interactions between them unique. The existence of bound dipole pairs, formed by two solitons with a $\pi$ phase shift, is worth being mentioned in this context [9]. Another important difference from solitons in media with local nonlinearity is the existence of repulsive forces between anisotropic solitons, if their distance and mutual orientation are properly chosen [10].

It was only recently that research focused on more complex structures than the nodeless ground modes. The step towards higher-order modes is a

* Corresponding author. Tel.: +49-6151-162279; fax: +49-6151-163279.
*E-mail address:* kristian.motzek@physik.tu-darmstadt.de (K. Motzek).

0030-4018/01/$ - see front matter © 2001 Published by Elsevier Science B.V.
PII: S0030-4018(01)01418-3

natural step in the direction of eventual use of solitons in data processing, because of the wide variety of possible interactions between them [11, 12]. For instance, a weak steering beam might not be able to deviate remarkably the trajectory of a strong beam, but a weak interaction between two components of a vector soliton might significantly change its internal structure. Again, the interaction of solitons in anisotropic media will differ from those in isotropic media.

The combination of a fundamental beam with a vortex beam cannot be a stationary solution in the anisotropic case. The vortex decays after a few diffraction lengths into a number of filaments, depending on its charge. We will show evidence of this in both our experimental and numerical investigations. Furthermore, it has been shown that vortex vector solitons are unstable even for an isotropic PR nonlinearity, though they can survive for long propagation distances before the vortex decays into a dipole [13,14]. Hence, the easiest way to obtain stable higher-order modes in anisotropic PR media seems to incoherently combine a fundamental beam with a dipole. However, to build a vector soliton, both beams have to be eigenmodes of their jointly induced waveguide. Dipole-mode vector solitons are believed to be stable in the isotropic case, although so far no rigorous proof has been offered. Numerical simulation, as well as experiment, indicate that they can survive for arbitrarily long propagation distances [13,14]. The purpose of this communication is to display the form, and the stability of dipole-mode vector solitons in anisotropic PR crystals going from weak dipole modes guided by the fundamental beam to multi-humped vector solitons and to cases where a strong dipole beam imposes its shape on the nodeless beam. In numerical simulations as well as in experiments the dipole-mode vector solitons showed no signs of instability throughout their entire existence region.

## 2. Theoretical description of photorefractive solitons

Neglecting absorption, the paraxial equations for the propagation of two beams along the $z$-axis read as follows [15]:

$$\begin{aligned} \partial_z U - \frac{\mathrm{i}}{2}\nabla_{\mathrm{T}}^2 U &= \mathrm{i}\gamma\,\partial_x\phi\, U, \\ \partial_z V - \frac{\mathrm{i}}{2}\nabla_{\mathrm{T}}^2 V &= \mathrm{i}\gamma\,\partial_x\phi\, V, \end{aligned} \tag{1}$$

where $U$ and $V$ are the slowly varying envelopes of the fundamental beam and the dipole, and $\nabla_{\mathrm{T}}$ is the transverse gradient. $\gamma = k^2 n_{\mathrm{e}}^2 x_0^2 r_{33}$ is the coupling constant, where $k$ is the wave number in the medium, $n_{\mathrm{e}}$ is the unperturbed refractive index, $x_0$ is the transverse scaling length and $r_{33}$ is the effective component of the electro-optic tensor. The propagation coordinate $z$ is measured in units of $z_0 = kx_0^2$. For our calculations we choose $x_0$ to be 12 μm. All other parameters were chosen corresponding to the experimental conditions described below, where light of wavelength $\lambda = 532$ nm, a SBN crystal with $r_{33} = 180$ pm/V and an externally applied electric field of 3.8 kV/cm were used.

The electrostatic potential $\phi$ appearing on the right hand side of Eq. (1) reflects the influence of the space charge field that builds up in the crystal, owing to the PR effect. The formation of this space charge is due to a change in the charge distribution inside the crystal which in turn is caused by the photoexcitation of electrons into the conduction band and their relocation outside the illuminated regions. The space charge field partially screens the externally applied electric field $E_0$, which is necessary for the creation of solitons, thus changing the refractive index of the material via the Pockels effect.

The $x$-axis is chosen to be in the direction of the external electric field. Using the Kukhtarev model equations to describe the material, the potential is found to satisfy the following differential equation [16]:

$$\begin{aligned} &\nabla^2\phi + \nabla \ln(1+I)\nabla\phi \\ &\quad = E_0\,\partial_x \ln(1+I) + (k_{\mathrm{B}}T/e)[\nabla^2 \ln(1+I) \\ &\qquad + (\nabla \ln(1+I))^2], \end{aligned} \tag{2}$$

where $I = |U|^2 + |V|^2$ is the total intensity, measured in the units of the saturation intensity $I_{\mathrm{d}}$, $k_{\mathrm{B}}$ is the Boltzmann constant, $e$ is the charge of the dominant carriers and $T$ is the temperature. In the following we shall neglect the diffusion terms (the terms proportional to $T$ on the right hand side

of Eq. (2)), which is justified for low temperatures. These terms cause self-bending of the light beams [17], but do not fundamentally change the shape and size of the solitary waves. The saturation intensity is another necessity for the formation of screening solitons. It reflects the fact that some electrons are always found in the conduction band. They are either thermally excited or lifted there by the background illumination.

We are interested in solitary solutions that do not change the transverse spatial distribution. Hence the ansatz:

$$\begin{aligned} U(x,y,z) &= u(x,y)\exp(\mathrm{i}\beta_1 z),\\ V(x,y,z) &= v(x,y)\exp(\mathrm{i}\beta_2 z). \end{aligned} \tag{3}$$

The intensity profiles of the beams remain unaltered throughout propagation, only their phases change, owing to the propagation constants $\beta_1$ and $\beta_2$. The constants reflect the change in the wave number due to the change in the refractive index caused by the beams. Inserting Eq. (3) into Eq. (1) we obtain the set of equations to be solved:

$$\begin{aligned} (\beta_1 - \tfrac{1}{2}\nabla_{\mathrm{T}}^2)u(x,y) &= \gamma\,\partial_x\phi(x,y)u(x,y),\\ (\beta_2 - \tfrac{1}{2}\nabla_{\mathrm{T}}^2)v(x,y) &= \gamma\,\partial_x\phi(x,y)v(x,y), \end{aligned} \tag{4}$$

which represents an eigenproblem akin to the Schrödinger equation, with the eigenvalues $\beta_1, \beta_2$ and the eigenfunctions $u, v$.

The solution of the problem is facilitated by the numerical method due to Petviashvili [18,19]. Fourier transforming Eq. (4) the problem changes into a fixed point equation:

$$\begin{aligned} u(\vec{k}_{\mathrm{T}}) &= \frac{\widehat{F}[\gamma\,\partial_x\phi\,u(x,y)](\vec{k}_{\mathrm{T}})}{\beta_1 + \vec{k}_{\mathrm{T}}^2/2},\\ v(\vec{k}_{\mathrm{T}}) &= \frac{\widehat{F}[\gamma\,\partial_x\phi\,v(x,y)](\vec{k}_{\mathrm{T}})}{\beta_2 + \vec{k}_{\mathrm{T}}^2/2}, \end{aligned} \tag{5}$$

where $\widehat{F}(\vec{k}_{\mathrm{T}})$ is the two dimensional Fourier transform in the transverse plane, and $\vec{k}_{\mathrm{T}}$ is the transverse wave vector.

Unfortunately, the simple iterations of Eq. (5) do not produce a numerical solution of the problem, but lead to divergence. To get convergence, the right hand sides of Eq. (5) have to be multiplied by the functionals $M_j^{\alpha}$ that leave the fixed points unaltered, according to the theory of fixed point equations. This is assured if $M_j[s_j(x,y)] = 1$, where $s_j(x,y)$ solves $(\beta_j - \frac{1}{2}\nabla_{\mathrm{T}}^2)s_j(x,y) = \gamma\,\partial_x\phi\,s_j(x,y)$, i.e. $s_1 = u$ and $s_2 = v$, however the convergence cannot be guaranteed. Petviashvili found nonetheless that

$$M_j = \frac{\int \mathrm{d}\vec{k}_{\mathrm{T}}\widehat{F}[\gamma\,\partial_x\phi\,s_j(x,y)](\vec{k}_{\mathrm{T}})\cdot s_j^*(\vec{k}_{\mathrm{T}})}{\int \mathrm{d}\vec{k}_{\mathrm{T}}(\beta_j + \vec{k}_{\mathrm{T}}^2/2)|s_j(\vec{k}_{\mathrm{T}})|^2} \tag{6}$$

achieves convergence, at least for the ground modes, provided $\alpha$ is chosen adequately. In our case $\alpha$ could have any value smaller than zero. The best results were obtained for $\alpha = -3/2$.

Our numerical procedure consists of the following. Choosing the initial functions $u_0$ and $v_0$ similar to the expected solution for $u$ and $v$, we iterate

$$\begin{aligned} u_{n+1}(\vec{k}_{\mathrm{T}}) &= |M_1|^{\alpha}\frac{\widehat{F}[\gamma\,\partial_x\phi\,u_n(x,y)](\vec{k}_{\mathrm{T}})}{\beta_1 + \vec{k}_{\mathrm{T}}^2/2},\\ v_{n+1}(\vec{k}_{\mathrm{T}}) &= |M_2|^{\alpha}\frac{\widehat{F}[\gamma\,\partial_x\phi\,v_n(x,y)](\vec{k}_{\mathrm{T}})}{\beta_2 + \vec{k}_{\mathrm{T}}^2/2}, \end{aligned} \tag{7}$$

calculating after each step the new potential $\phi$ from Eq. (2). The iteration stops when the relative error gets smaller than $10^{-5}$ in both components. The initial beams are chosen as the simple Gaussian for the fundamental, and a pair of Gaussians, with a $\pi$ phase shift between them, for the dipole. The stability of the results thus obtained was checked by numerically propagating the vector solitons for 10 diffraction lengths, using our programs for the integration of full Eqs. (1) and (2). All the results concerning a nodeless beam and a dipole perpendicular to the externally applied field proved to be stable.

## 3. Dependency on propagation constants

We focus on the effects of combined propagation of the fundamental beam ($u$-component) and the dipole beam ($v$-component). The dipole is oriented perpendicular to the externally applied electric field. To see how the vector solitons change when the intensity of one beam is increased relative to the other, we choose a fixed propagation constant $\beta_1$ for the fundamental beam and vary $\beta_2$.

In experiment, changing the value of the propagation constant corresponds to changing the initial beams' intensity.

The first result reveals the existence of a lower and an upper cutoff value $\beta_2^{\min}$ and $\beta_2^{\max}$ for the propagation constant $\beta_2$. Dipole-mode vector solitons exist for all $\beta_2$ between these two values, but none are found outside of this range. For all fixed values of $\beta_1$ used, $\beta_2^{\min}$ was always slightly bigger than $\beta_1/4$ and $\beta_2^{\max} \approx \beta_1$. An explanation for this behavior can be extracted from the further analysis of vector solitons.

Fig. 1 depicts the integrated intensity of the vector soliton and of the two beams comprising it. As can be seen, the dipole intensity gets smaller as $\beta_2$ decreases, until apparently it reaches zero for $\beta_2 = \beta_2^{\min}$. (Our numerical procedure converges poorly for $\beta_2$ very close to the cutoff values, so we could not determine them exactly.) In this case the vector soliton changes into a scalar soliton. For the values of $\beta_2$ close to the lower cutoff value the dipole intensity is so small, that its own waveguide can be neglected in the first approximation (for a weak beam the refractive index modulation is proportional to the intensity). We can then regard the vector soliton as a scalar soliton that guides a weak dipole beam. Since the intensity profile of the dipole cannot change during propagation, it has to be an eigenmode of the waveguide induced by the scalar soliton. As shown in Fig. 2(a), the fundamental beam intensity profile is indeed very similar to a scalar soliton intensity profile, provided the scalar soliton has the propagation constant $\beta = \beta_1$. This explains the existence of the lower cutoff value.

A vector soliton can exist as long as both beams are eigenmodes of the jointly induced waveguide. Therefore, if one of the beams is too weak to significantly change the waveguide, as in the case of Fig. 2(a) the dipole is, i.e. if the total intensity profile of the vector soliton is almost identical to the intensity profile of the fundamental beam, then the fundamental beam has to be an eigenmode of itself, i.e. a scalar soliton. Furthermore, the dipole has to be an eigenmode of the waveguide induced by this scalar soliton. In other words, in the limiting case when the dipole intensity is vanishingly small, its propagation constant is equal to the propagation constant of the dipole eigenmode of a waveguide induced by the scalar soliton, and this propagation constant is equal to $\beta_2^{\min}$. The reason

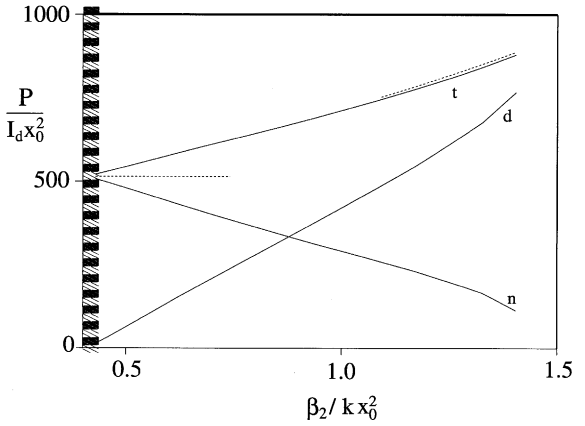


Fig. 1. Integrated intensity of the soliton versus the propagation constant $\beta_2$, for $\beta_1 = 1.55kx_0^2$. The line marked with $n$ is the nodeless beam intensity, $d$ stands for the dipole intensity and the line marked with $t$ is the sum of both. The dotted lines show the asymptotics. For the lower values of $\beta_2$ the total integrated intensity converges to the intensity of a scalar soliton with the propagation constant $\beta = \beta_1$ (horizontal dotted line). For the higher values of $\beta_2$ the total intensity approaches the intensity of a bound dipole pair with the propagation constant $\beta = \beta_2$ (diagonal dotted line).

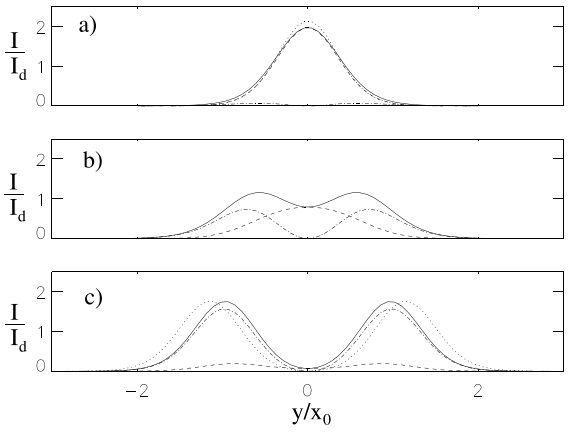


Fig. 2. Profiles of the three vector solitons with $\beta_1 = 1.55$. $\beta_2$ is 0.47 in (a), 0.94 in (b) and 1.40 in (c). The solid line represents the total intensity, the dashed line the fundamental beam, and the dash-dotted line the dipole. The dotted line in (a) represents the limiting case of a scalar soliton, and in (c) the limiting case of a bound dipole pair.

why the lower cutoff value $\beta_2^{\min} \approx \beta_1/4$ over a wide range of fixed values of $\beta_1$, is that the waveguide induced by the scalar soliton does not change its form significantly as the soliton propagation constant is changed. Therefore, the form of the higher eigenmodes of this waveguide does not change significantly either.

Going to higher values of $\beta_2$ the dipole intensity keeps growing, while the fundamental beam intensity decreases. Midway between the cutoff values the vector nature of the soliton becomes apparent: without the presence of the other component, either beam would change under propagation. The intensity profile of the vector soliton takes a form that does not resemble any scalar soliton, eventually having two maxima, as shown in Fig. 2(b). A further investigation into the interaction of such solitons with other vector or scalar solitons is needed.

As $\beta_2$ approaches $\beta_2^{\max}$ the integrated intensity of the fundamental beam gets smaller, until it apparently reaches zero for $\beta_2 = \beta_2^{\max}$. In this case, similar to the above, the vector soliton changes into a scalar dipole soliton, i.e. into a coherent pair of scalar solitons with a $\pi$ phase shift between them, forming a bound dipole pair, as described in Ref. [9]. For $\beta_2 \approx \beta_2^{\max}$ the fundamental beam intensity is so small that its influence on the waveguide can be neglected. This is then a weak nodeless beam guided by a bound dipole pair, the nodeless beam being an eigenmode of the waveguide induced by the dipole pair. If $\beta_2$ is now chosen such that a bound dipole pair with this propagation constant has an internal fundamental eigenmode with a propagation constant equal to $\beta_1$, the two constants are close to each other, and we have found $\beta_2^{\max}$. In this case, as shown in Fig. 2(c), the shape of the fundamental beam intensity distribution adopts more and more to the dipole, showing two maxima. This explains why the upper cutoff value $\beta_2^{\max} \approx \beta_1$. If a waveguide induced by the dipole guides the fundamental beam, then the shape of the latter will look like the dipole, except in the region of $\pi$ phase shift. Therefore, a weak fundamental beam guided by a dipole with the propagation constant $\beta_2$ will have a propagation constant close to $\beta_2^{\max}$. As mentioned earlier, the existence of bound dipole pairs is a feature of anisotropic PR media that has no counterpart in the isotropic case.

An insight into the physical meaning of propagation constants can also explain why the integrated intensity of the dipole component increases and the intensity of the fundamental component decreases with growing $\beta_2$. Since the propagation constants reflect an increase in the refractive index caused by the beams, $\beta_2$ can only grow if the refractive index increases in the regions where the dipole has its maxima, i.e. if the intensity of the dipole increases. On the other hand, this means that the intensity in the center of the vector soliton has to decrease, in order to keep the fundamental beam propagation constant $\beta_1$ fixed, i.e. the intensity of the fundamental beam has to decrease.

From the above we conclude that for $\beta_2 = \beta_2^{\min}$ the $u$-component of the vector soliton has the shape and size of a scalar ground mode with the propagation constant $\beta = \beta_1$, while the $v$-component is 0. For the upper cutoff $\beta_2 = \beta_2^{\max}$ the $u$-component is 0, while the $v$-component is a bound dipole pair, as described by Mamaev et al. [9], with $\beta = \beta_2$. Both limiting cases are confirmed by Fig. 2(a) and (c), where the calculated shapes of the vector solitons close to the lower and upper cutoff values are compared to the single soliton with the propagation constant $\beta = \beta_1$ and to the bound dipole pair with the propagation constant $\beta = \beta_2$, respectively.

## 4. Comparison of theoretical and experimental results

Figs. 3 and 4 show how the vector solitons change when the ratio of the fundamental beam intensity to the dipole beam intensity is altered. Fig. 3 depicts the numerically obtained solitary solutions. The propagation constants $\beta_1$ and $\beta_2$ were chosen to yield vector solitons with a total integrated intensity of 700 in units of $1/(I_d x_0^2)$, which corresponds to the laser powers used in the experiment described below. A readily observed effect is that the nodeless beam gets stretched along the $y$-axis, as the power ratio of the nodeless beam to the dipole beam, $P_n/P_d$, gets smaller. Furthermore, the distance between the two maxima of the

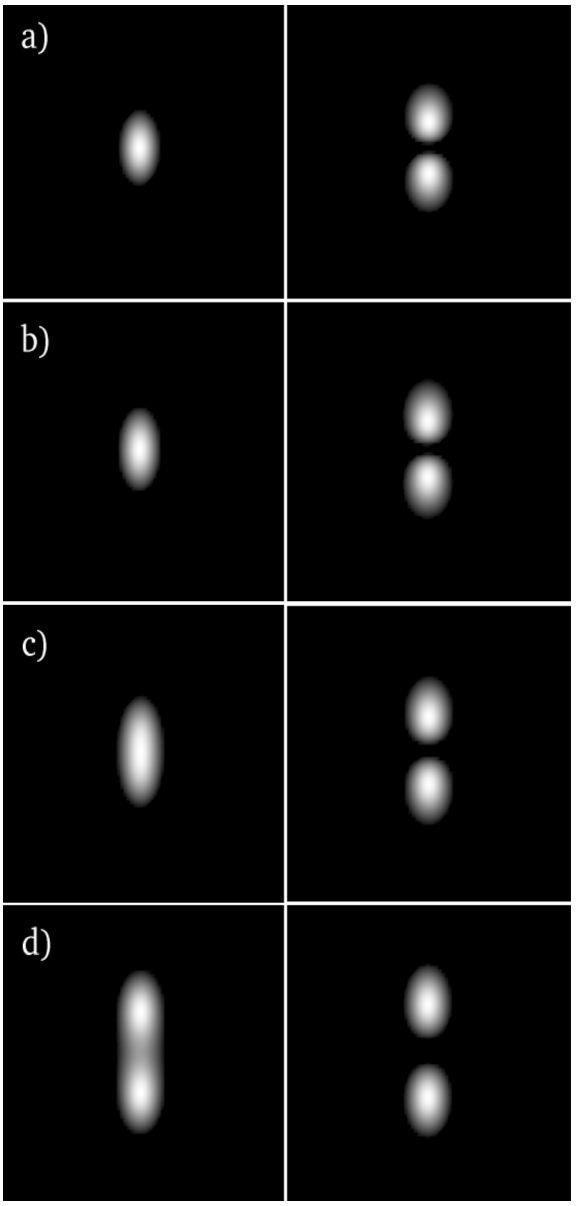


Fig. 3. Calculated intensity distributions for vector solitons with an integrated intensity of 700 measured in units of $I_d x_0^2$. Left column the fundamental beam, right column the dipole. The ratio of the fundamental beam integrated intensity to the dipole integrated intensity is 3.6 in (a), 1.7 in (b), 0.67 in (c) and 0.22 in (d).

dipole beam increases (by about 20% from Fig. 2(a)–(c)). The latter effect is more clearly seen in the profile plot of the dipole beam in Fig. 2. This is

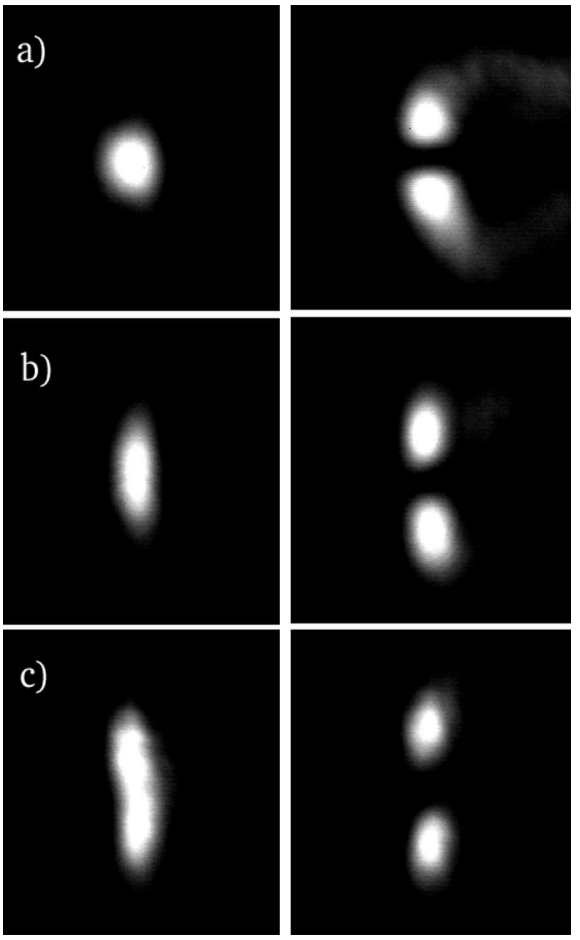


Fig. 4. Experimental figures of vector solitons with the total integrated intensity of 3 μW: (a), (b) and (c) as in Fig. 3.

in qualitative agreement with Fig. 4, which presents experimental data.

The experiment is performed using a SBN crystal measuring $13.5 \times 5 \times 5$ mm$^3$ ($a \times b \times c$) with an externally applied electric field of 3.8 kV/cm along the $c$-axis. The setup is basically described in Ref. [14]. The beams propagated 5 mm inside the crystal. The total intensity of the two beams was 3 μW and light from a Nd:YAG laser ($\lambda = 532$ nm) was used. Obviously the two effects described above, the stretching of the fundamental beam and the growing separation of the dipole maxima, resulting from a decreased value of $P_n/P_d$, are confirmed by the experiment. As far as the separation of the dipole beam maxima is con-

cerned, the effect is much more pronounced in the experiment than predicted by the numerical results.

In order to verify if setting the temperature to zero in Eq. (2) limits the validity of our theoretical results, we let our computationally obtained solitary solutions to Eq. (4) propagate numerically for 10 diffraction lengths, with the temperature $T$ in Eq. (2) set to 300 K. As expected self-bending occurred, but the beams' intensity profiles did not change under propagation. That is, the numerical solitary solutions discussed above hold also for temperatures typically encountered in experimental setups.

## 5. Conclusion

In conclusion, we have investigated the behavior of dipole-mode vector solitons in anisotropic PR media when the ratio of the dipole beam's intensity to the nodeless beam's intensity is varied, with the dipole directed perpendicular to the externally applied field. It was shown that these vector solitons form a continuous set of solutions to the propagation equations, ranging from the limiting case of single scalar solitons, to the limiting case of bound dipole pairs. Both limiting cases were found to be stable in numerical simulation, as well as in experiment, and the intermediate case of a vector soliton (having one or two maxima) also proved to be a stable entity in both numerical and experimental propagation.

## References

[1] M. Segev, Opt. Quant. Electron. 30 (1998) 503.
[2] M. Segev, B. Crosignani, A. Yariv, B. Fischer, Phys. Rev. Lett. 68 (1992) 923.
[3] J.E. Bjorkholm, A. Ashkin, Phys. Rev. Lett. 32 (1974) 129.
[4] D.E. Pelinovsky, A.V. Buryak, Y.S. Kivshar, Phys. Rev. Lett. 75 (1995) 591.
[5] C. Denz, W. Królikowski, J. Petter, C. Weilnau, M.R. Belić, F. Kaiser, A. Stepken, Phys. Rev. E 60 (1999) 6222.
[6] A. Stepken, F. Kaiser, M.R. Belić, J. Opt. Soc. Am. B 17 (2000) 68.
[7] S. Gatz, J. Herrmann, IEEE J. Quant. Electron. 28 (1992) 1732.
[8] A.W. Snyder, A.P. Sheppard, Opt. Lett. 18 (1993) 482.
[9] A.V. Mamaev, A.A. Zozulya, V.K. Mezentsev, D.Z. Anderson, M. Saffman, Phys. Rev. A 56 (1997) 1110.
[10] A. Stepken, F. Kaiser, M.R. Belić, W. Królikowski, Phys. Rev. E 58 (1998) 4112.
[11] Z.H. Musslimani, M. Soljačić, M. Segev, D.N. Christodoulides, Phys. Rev. Lett. 86 (2001) 799.
[12] J.J. García-Ripoll, V.M. Pérez-García, W. Królikowski, Y.S. Kivshar, arXiv:nlin.PS/0006047.
[13] J.J. García-Ripoll, V.M. Pérez-García, E.A. Ostrovskaya, Y.S. Kivshar, Phys. Rev. Lett. 85 (2000) 82.
[14] W. Krolikowski, E.A. Ostrovskaya, C. Weilnau, M. Geisser, G. McCarthy, Y.S. Kivshar, C. Denz, B. Luther-Davies, Phys. Rev. Lett. 85 (2000) 1424.
[15] D.N. Christodoulides, M.J. Carvalho, J. Opt. Soc. Am. B 12 (1995) 1628.
[16] A.A. Zozulya, D.Z. Anderson, Phys. Rev. A 51 (1995) 1520.
[17] J. Petter, C. Weilnau, C. Denz, A. Stepken, F. Kaiser, Opt. Commun. 170 (1999) 291.
[18] V.I. Petviashvili, Fiz. Plazmy 2 (1976) 469.
[19] A.A. Zozulya, D.Z. Anderson, A.V. Mamaev, M. Saffman, Phys. Rev. A 57 (1998) 522.